Eur J Nucl Med Mol Imaging (2010) 37:1377–1385
DOI 10.1007/s00259-009-1379-3

ORIGINAL ARTICLE

Assessment of the Na/I symporter as a reporter gene to visualize oncolytic adenovirus propagation in peritoneal tumours

Andrew Merron · Patrick Baril · Pilar Martin-Duque · Antonio de la Vieja · Lucile Tran · Arnaud Briat · Kevin J. Harrington · Iain A. McNeish · Georges Vassaux

Received: 23 July 2009 / Accepted: 24 December 2009 / Published online: 6 February 2010

Abstract
Purpose In vivo imaging of the spread of oncolytic viruses using the Na/I symporter (NIS) has been proposed. Here, we assessed whether the presence of *NIS* in the viral genome affects the therapeutic efficacy of the oncolytic adenovirus *dl922-947* following intraperitoneal administration, in a mouse model of peritoneal ovarian carcinoma.
Methods We generated AdAM7, a *dl922-947* oncolytic adenovirus encoding the *NIS* coding sequence. Iodide uptake, NIS expression, infectivity and cell-killing activity of AdAM7, as well as that of relevant controls, were determined in vitro. In vivo, the propagation of this virus in the peritoneal cavity of tumour-bearing mice was determined using SPECT/CT imaging and its therapeutic efficacy was evaluated.
Results In vitro infection of ovarian carcinoma IGROV-1 cells with ADAM7 led to functional expression of NIS. However, the insertion of *NIS* into the viral genome resulted in a loss of efficacy of the virus in terms of replication and cytotoxicity. In vivo, on SPECT/CT imaging AdAM7 was only detectable in the peritoneal cavity of animals bearing peritoneal ovarian tumours for up to 5 days after intraperitoneal administration. Therapeutic experiments in vivo demonstrated that AdAM7 is as potent as its NIS-negative counterpart.
Conclusion This study demonstrated that despite the detrimental effect observed in vitro, insertion of the reporter gene *NIS* in an oncolytic adenovirus did not affect its therapeutic efficacy in vivo. We conclude that *NIS* is a highly relevant reporter gene to monitor the fate of oncolytic adenovectors in live subjects.

Keywords Molecular imaging · Oncolytic adenovirus · Na/I symporter · SPECT/CT · Gene therapy

A. Merron · I. A. McNeish
Centre for Molecular Oncology, Institute of Cancer,
Queen Mary's School of Medicine and Dentistry,
London, UK

P. Baril · L. Tran · G. Vassaux (✉)
INSERM U948, CHU Hôtel Dieu,
1 place Alexis Ricordeau,
44035 Nantes Cedex1, France
e-mail: georges.vassaux@inserm.fr

P. Baril · L. Tran · G. Vassaux
Institut des Maladies de l'Appareil Digestif, CHU de Nantes,
Nantes, France

P. Martin-Duque
I+CS/ Araid Fund, Instituto Aragonés de Ciencias de la Salud,
Zaragoza, Spain

A. de la Vieja
Instituto de Investigaciones Biomédicas "Alberto Sols" C/Arturo
Duperier 4,
Madrid, Spain

A. Briat
INSERM U877,
Grenoble, France

K. J. Harrington
Institute of Cancer Research, Chester Beatty Laboratories,
London, UK

Introduction

The Na/I symporter (NIS) gene is endogenously expressed in the thyroid and stomach, and to a lesser extent in the salivary glands, breast and thymus [1]. In the thyroid, NIS is responsible for the uptake and concentration of iodine [1]. For this, NIS uses the sodium gradient generated from the Na^+/K^- ATPase to cotransport two Na^+ ions and one I^-

ion across the basolateral membrane of thyroid follicular cells. NIS expression and function are also key to the successful treatment of differentiated thyroid carcinomas with $^{131}I^{-}$ [2]. In nonthyroidal tissues, ectopic expression of NIS through gene transfer can lead to iodine uptake that can be imaged noninvasively [2–4]. The imaging of NIS-expressing tissues is particularly versatile since NIS can promote cellular uptake of different radioisotopes: $^{123}I^{-}$, $^{99m}TcO_4^{-}$ (visualized using single photon emission computed tomography, SPECT), $^{124}I^{-}$ (visualized using positron emission tomography, PET), and $^{131}I^{-}$ (visualized using scintigraphy) [5–13]. In term of applications, NIS imaging has been used to visualize the activation of specific signalling pathways or promoters [14–19] and the viability of cells with therapeutic potential [20], and is a relevant reporter gene for myocardial gene transfer [21] and cancer gene therapy [5, 22–25]. Very recently, the use of this reporter gene has been validated in humans [26].

Replication-competent 'oncolytic adenoviruses' have been used extensively in cancer therapy [27]. Their appeal resides in the fact that they are designed to replicate selectively in cancer cells. This self-amplification results in the spread of the virus in the tumour, leading to an improved therapeutic efficacy [28]. One strategy proposed to engineer oncolytic viruses is a 24-bp deletion in the adenoviral E1A gene [29, 30]. This deletion renders the resulting protein unable to bind the tumour-suppressor Rb. As a result, a virus carrying this deletion (*dl922-947*) is unable to replicate in and kill cells with a normal Rb pathway, but can trigger cytotoxicity in cancer cells with a disrupted Rb pathway. Based on this principle, *dl922-947* has been shown to be effective against experimental glioma [29, 30]. More recently, intraperitoneal administration of *dl922-947* to mice bearing intraperitoneal ovarian carcinoma has demonstrated that *dl922-947* is active against this tumour-type [31]. Interestingly, *dl922-947* is more potent than other adenoviral mutants (*dl309* or *dl1520*) and than the parental, adenovirus 5 wild-type. Administration of the virus in a α-1, 4-linked glucose polymer (icodextrin) instead of phosphate-buffered saline (PBS) further increases the therapeutic efficacy, probably due to the increased half-life of the virus in the peritoneal cavity [31]. Considering that intraperitoneal administration is more amenable to systemic spread than intratumoral injection, arming *dl922-947* with a reporter gene with potential applications in humans would be of interest to monitor viral spread and biodistribution over time.

The utilization of *NIS* as a reporter gene to visualize the propagation of oncolytic viruses in tumours has been validated for oncolytic measles viruses [32] and adenoviruses [9, 25]. In the latter case, the insertion of *NIS* has been shown to have beneficial effects on the cytotoxicity of the virus in primary desmoid tumour cells in vitro [33]. In the present study, we investigated the impact of the presence of *NIS* in the *dl922-947* adenovirus and, in particular, assessed whether the presence of *NIS* as a reporter gene could affect the therapeutic efficacy of *dl922-947* in in vivo observations following intraperitoneal administration of the virus in a mouse model of ovarian carcinoma.

Materials and methods

Generation and production of a *dl922-947* adenovirus encoding *NIS*

The plasmids encoding the genomes of the oncolytic viruses used in this study were generated by homologous recombination in yeast, using a methodology similar to that described previously [9, 25, 34–36]. The detail of the construction of the viruses is available from the corresponding author upon request. The presence of NIS and the deletion *dl922-947* in the E1 locus were verified by sequencing. Virus were produced and titrated as previously described [36, 37].

Adenovirus nomenclature

- AdGFP: Replication-deficient adenovirus type 5 encoding the green fluorescent protein as a transgene [38].
- AdAM7: Adenovirus carrying the *dl922-947* deletion and in which the gp19k/6.7 genes in the E3 region of the adenoviral genome have been replaced by the *NIS* coding sequence.
- AdAM8: Adenovirus carrying the *dl922-947* deletion and in which the gp19k/6.7 genes in the E3 region of the adenoviral genome have been deleted. This *NIS*-negative virus acts as a control of AdAM7.

Cell lines

The cell lines IGROV-1 and IGROV-luc were used in this study and were obtained and cultured as previously described [31].

Infection with adenoviruses

Cells were seeded at a cell density of 10^4 cells/cm^2. The following day they were infected with adenoviruses at different multiplicities of infection (MOI) in serum-free medium for 30 to 45 min. Culture medium was then added to reach a serum concentration of up to 20%.

Biochemical assays and immunohistochemistry

Cell survival assays, assessment of in vitro viral replication, iodine uptake and E1A expression were performed as previously described [9, 10, 12].

Animals

All experiments were conducted with appropriate ethical approval and in accordance with the United Kingdom "Guidance on the operation of animals (Scientific Procedure) Act 1986" (HMSO, London, 1990). BALB/c nu/nu mice at 6–8 weeks of age were obtained from Harlan (UK), allowed to acclimatize for 1 week, and for the duration of the experiments were kept in individualised ventilated cages and given food and water ad libitum. IGROV-luc cells (3×10^6) were injected intraperitoneally in BALB/c nu/nu mice. Mice were then assessed daily for weight, general health and accumulation of ascites. Tumour burden is proportional to luciferase activity [31]. Luciferase activity was measured as previously described [39, 40].

NanoSPECT/CT imaging

Animals were anaesthetized and then given an intravenous injection of 18.5 MBq of $^{99m}TcO_4^-$. Mice were then placed onto a sealed, prewarmed (37°C) mouse bed of the SPECT/CT scanner (Bioscan, Washington DC) connected to gas anaesthetic (600–800 cm^3/min N_2O, 1 l/min O_2 and 1.5–2% v/v halothane) delivery and scavenging system. To improve reproducibility, mice were scanned routinely 10 min after $^{99m}TcO_4^-$ injection. Mice were imaged as follows. A topogram of the entire mouse bed was acquired to determine the limits of the SPECT/CT scan of the mouse to be imaged. The CT scan was performed first, followed by the SPECT acquisition using the limits set by the topogram. The time of acquisition of the CT scan depended on the size of the scan (as determined by the topographic limits of the scan) and on the total activity of the radiotracer injected. In any case, the total scanning time (SPECT and CT) never exceeded 30 min. SPECT acquisition collected 100,000 counts per projection, using a 16-projection and four-pinhole system. After CT and SPECT acquisitions, a blank scan was taken and the mouse was removed from the scanner and allowed to recover in a warm darkened environment.

SPECT and CT scan data were reconstructed using the MEDISO software package (Medical Imaging Systems). SPECT and CT images were comerged and fused using PMOD software (PMOD Technologies). Radioisotope accumulation was quantified using InVivoScope software (Medical Imaging Systems) by drawing voxel-guided specific volumes of interest using the fused SPECT/CT images. Radioisotope accumulation was expressed as the total amount of radioactivity (MBq) divided by the total activity injected into the mouse (MBq) divided by the volume of quantification (mm^3). In the kinetic study presented in Fig. 4, this procedure (anaesthesia, $^{99m}TcO_4^-$ injection, data acquisition, quantification and analysis) was repeated every day.

Statistical analysis

Statistical analysis was performed using Prism (GraphPad software). Dual comparisons were made using the Student's *t*-test and comparison between multiple conditions were analysed using ANOVA.

Results

Na/I symporter expression in vitro

To determine whether infection of the ovarian carcinoma IGROV-1 cells with the *dl922-947* adenovirus encoding *NIS* (AdAM7) leads to NIS expression, immunocytochemistry was performed on IGROV-1 cells infected with AdAM7. Figure 1a shows AdAM7 dose-dependent NIS immunoreactive staining essentially at the membrane of the cells. In some cells, immunoreactive signal could also be detected in the cytosol of the cells (*C* in Fig. 1a). To determine whether NIS was functional, an in vitro iodide uptake assay was performed. AdAM7 infection induced a dose-dependent iodide uptake that could be inhibited with the NIS-selective inhibitor perchlorate. As a control, the same experiments performed with the NIS-negative *dl922-947* adenovirus (AdAM8) failed to show NIS immunoreactivity of IGROV-1 cells as well as iodide uptake (not shown). Taken together, these findings demonstrate that infection of IGROV-1 cells with AdAM7 leads to a functional expression of NIS protein.

Effect of NIS expression on replication and cytotoxicity of *dl922-947* adenovirus

Analysis of the adenoviral protein E1A expression 24 h after infection of IGROV-1 cells with either AdAM7 or AdAM8 led to a strong E1A-specific immunoreactivity (Fig. 2), indicating that both viruses were equally infective. As expected, this staining was absent in IGROV-1 cells infected with a replication-deficient E1A-negative AdGFP (Fig. 2). To compare the replicating potential of AdAM7 and AdAM8, cells were infected on day zero and the kinetics of virus production were established. The virus yield in AdAM7- and AdAM8-infected IGROV-1 cells peaked 2–3 days after infection (Fig. 3a). The yield of

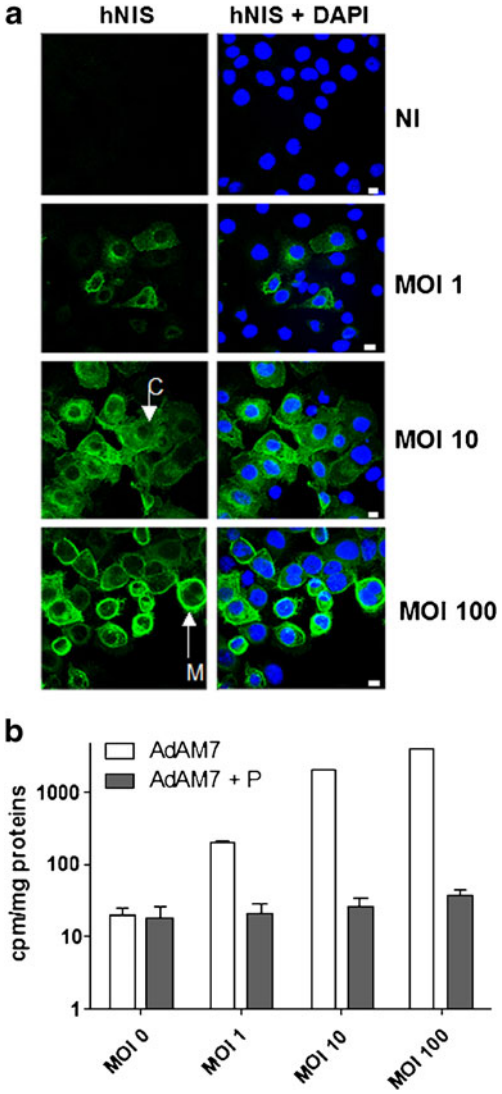

Fig. 1 NIS expression following infection of IGROV-1 cells with AdAM7. IGROV-1 cells were infected at different MOIs of AdAM7 and processed 24 h later (*NI* noninfected). **a** Immunocytochemistry with a NIS-specific antibody (*M* immunoreactive signal at the cell membrane, *C* immunoreactive signal in the cytosol). The results presented are representative of two independent experiments (*bars* 1 μm). **b** Iodine uptake. The results presented (means±SD) were obtained in one experiment, representative of two other independent experiments (*P* NIS inhibitor sodium perchlorate, 100 μ*M*)

infective adenoviral particles produced in IGROV-1 cells infected with the *NIS*-negative virus AdAM8 was far greater (more than two orders of magnitude, $p<0.0001$) than that produced in IGROV-1 cells infected with AdAM7. These results suggest that the presence of NIS in the adenoviral genome impairs the replication of replication-selective oncolytic *dl922-947* adenovirus.

To determine the impact of the presence of *NIS* in the viral genome on the cytotoxicity of the viruses, AdAM7 and AdAM8 were used to infect IGROV-1 cells and the metabolic activity was measured as a reflection of the number of live cells 96 h later. Infection with AdAM8 led to dose-dependent cytotoxicity that was superior to that of AdAM7 when MOIs of 10 or 100 were used (in both cases, AdAM8 versus AdAM7, $p<0.001$). However, at low MOI (MOI of 1), the difference between the two viruses was not statistically significant ($p>0.05$). As a control, infection of IGROV-1 cells with the replication-deficient AdGFP led only to mild toxicity at high MOIs (Fig. 3b). Similar data were obtained using IGROV-1 cells expressing the luciferase gene (not shown), a stable cell line obtained by transduction of these cells with a lentivirus encoding the luciferase gene [31].

Imaging in vivo

Biodistribution of NIS expression following intraperitoneal administration of AdAM7 to IGROV-luc tumour-bearing mice in the presence of icodextrin was monitored by SPECT/CT over time. In these experiments, $^{99m}TcO_4^-$ was used as the radioactive tracer. As expected from the endogenous expression of NIS in the thyroid glands and the stomach, $^{99m}TcO_4^-$ accumulation was detectable in these organs. The bladder was also visible, as a result of excretion of $^{99m}TcO_4^-$ in the urine (Fig. 4). An additional signal was detected in the peritoneal cavity, corresponding to IGROV-luc tumour cells infected with AdAM7 (Fig. 4). Careful analysis of the tomographic images failed to reveal $^{99m}TcO_4^-$ accumulation in any other anatomical location. Quantitative analysis of the images revealed that $^{99m}TcO_4^-$ accumulation in the peritoneal cavity was maximal 48 h after virus administration and gradually decreased afterwards. By day 8, no accumulation of $^{99m}TcO_4^-$ above background was detectable (Fig. 5). As expected, when AdAM8 was administered to a parallel cohort of IGROV-luc tumour-bearing mice, $^{99m}TcO_4^-$ accumulation was detected in the thyroid, stomach and bladder, but no additional signal was observed (Fig. 4).

Therapeutic effect in vivo

The growth of IGROV-luc cells can be monitored in vitro through the measurement of luciferase activity in the culture [31]. In vivo, intraperitoneal injection of IGROV-luc cells leads to the establishment of disseminated peritoneal tumours and bioluminescent imaging can be used to monitor tumour burden over time [31]. We compared the therapeutic effects of AdAM7 and AdAM8. IGROV-luc cells were injected intraperitoneally on day 0 and the viruses were administered on day 4. At this time-point, the tumour burden, as measured by luciferase activity was homogenous ($7\times10^7 \pm 10^6$ light units per mouse). Administration of either virus resulted in a slow reduction in luciferase activity, and the peak therapeutic effect was on

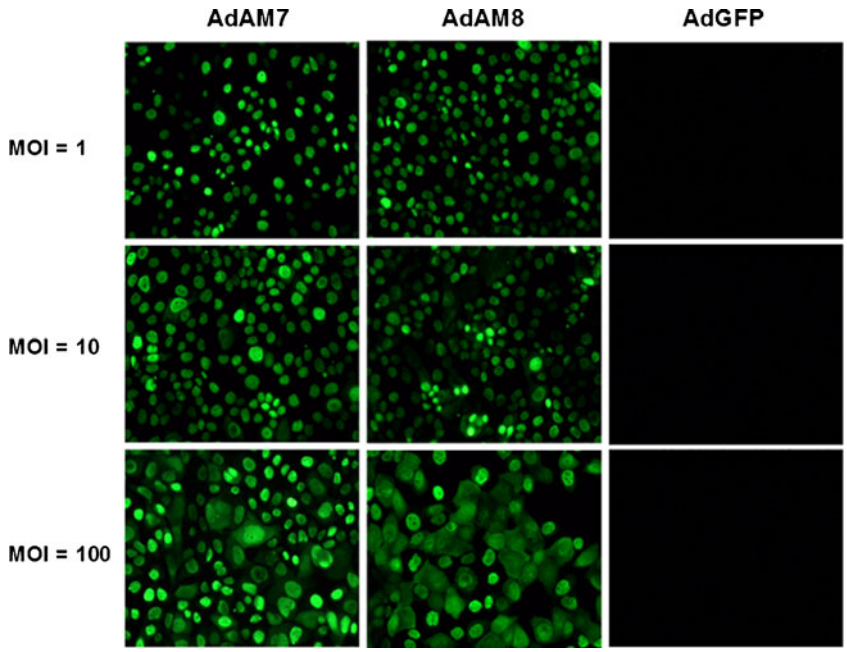

Fig. 2 E1A expression following infection of IGROV-1 cells with AdAM7, AdAM8 or AdGFP. IGROV-1 cells were infected at different MOIs of AdAM7, AdAM8 or AdGFP. The cells were processed 24 h later for immunocytochemistry using an E1A-specific antibody. The results presented are representative of two independent experiments

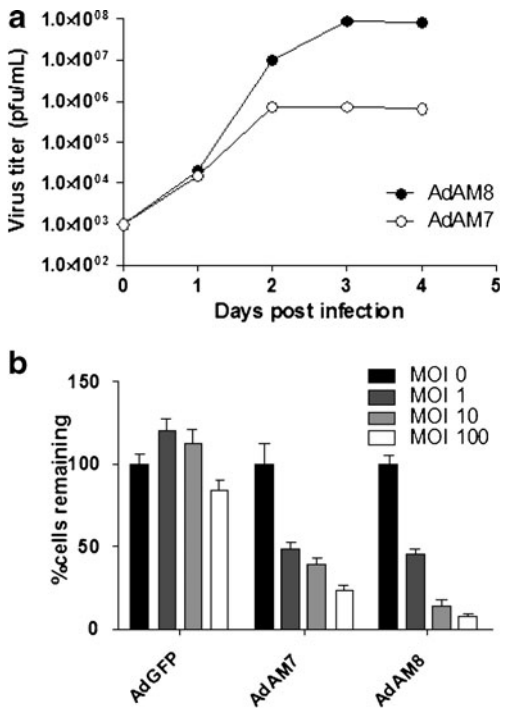

Fig. 3 Replication and oncolytic activity of AdAM7 and AdAM8 in IGROV-1 cells. IGROV-1 cells were infected with virus at an MOI of 5 (**a**) or at different MOIs (**b**). **a** The cells were collected daily after infection and the viral content of the homogenates was determined by titration. The experiment presented is representative of three independent experiments performed in triplicate (the data are means±SD of the triplicate determinations). **b** Cell viability was measured 5 days after infection using the MTT assay. The data are expressed as percentages of the value obtained in the noninfected control wells (100%), and are representative of three independent experiments performed in triplicate (means±SD of the triplicate determinations)

day 11 (Fig. 6). At this time-point, the luciferase activity was significantly different from that of animals treated with PBS (p=0.02). From day 12, the tumour burden increased again, demonstrating the lack of efficacy of a single viral vector administration in this model. No statistically significant differences were observed between the antitumour activities of AdAM7 and AdAM8 (p>0.05). These results suggest that despite the difference in potency in vitro, both viruses are equally potent in vivo.

Discussion

The potential of the oncolytic adenovirus *dl922-947* for the treatment of ovarian cancer has already been validated [31, 41], and intraperitoneal coinjection of this virus with icodextrin instead of PBS further increased therapeutic efficacy [31]. Translating this approach to ovarian cancer is therefore tempting. However, considering that intraperitoneal injection of adenovirus leads to liver [42, 43] and prostate transduction [42] in rodents, imaging oncolytic virus biodistribution in patients would provide unique data relevant to the biosafety and efficacy of the treatment. In this context, and considering that NIS imaging is possible in humans following adenovirus injection [26], arming oncolytic adenovirus with NIS is an attractive approach.

In the present study, we assessed the impact of the presence of *NIS* in the *dl922-947* adenovirus and in particular assessed whether the presence of *NIS* as a reporter gene could reduce the therapeutic efficacy of *dl922-947*. In vitro, AdAM7 (*dl922-947* oncolytic adeno-

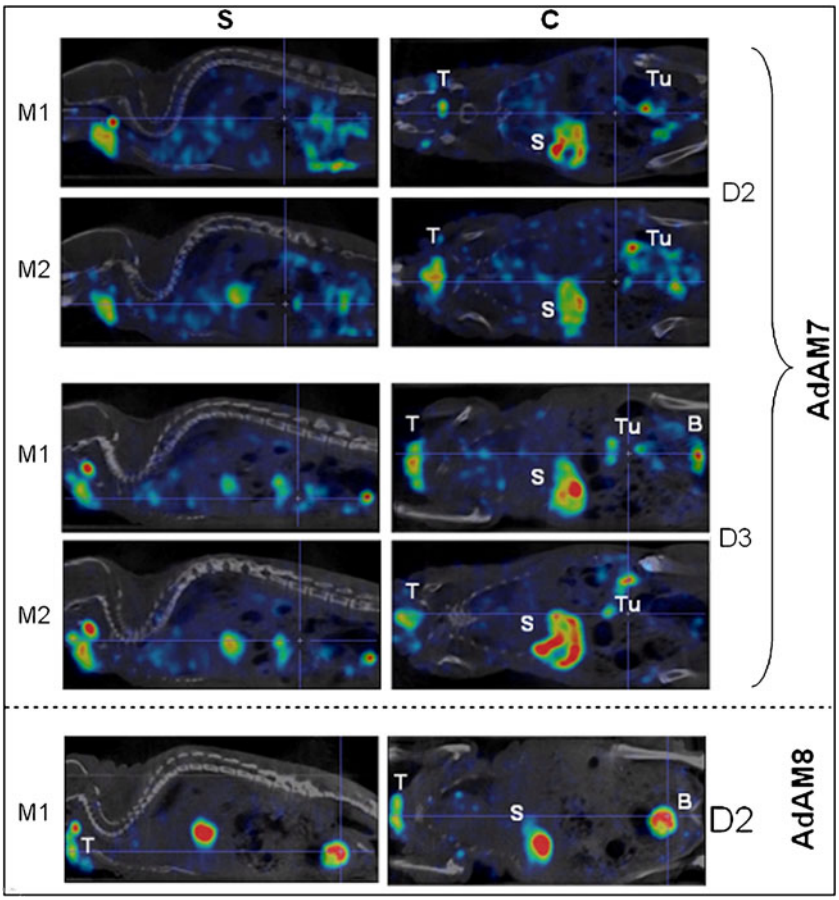

Fig. 4 Propagation of AdAM7 in peritoneal IGROV-luc tumour deposits. Balb-c nude mice were seeded intraperitoneally with IGROV-luc cells. The mice were injected 2 days later with PBS (n=3), 10^{10} particles of AdAM7 (n=4) or AdAM8 (n=2). Mice were scanned using a dedicated small-animal SPECT/CT scanner and representative sections showing $^{99m}TcO_4^-$ accumulation in the peritoneal cavity (days 2 and 3) are presented (*S* sagittal section, *C* coronal section; *D2* day 2, *D3* day 3, *M1* mouse 1, *M2* mouse 2; *B* bladder, *S* stomach, *T* thyroid, *Tu* tumour)

virus encoding *NIS*) was able to infect IGROV-1 cells as efficiently as AdAM8 (*dl922-947* oncolytic adenovirus without *NIS*; Figs. 2 and 3) but the yield of virus following AdAM7 infection was inferior and, probably as a result, this virus exerted a lower cytotoxic effect on IGROV-1 cells (Fig. 3b). These findings suggest that introduction of *NIS* as a reporter gene into an oncolytic adenovirus would have a detrimental effect on its oncolytic activity in vitro. The expression of *NIS* from a replication-incompetent adenovirus has not been reported to be associated with particular side effects [10] in established cancer cell lines including IGROV-1 cells (not shown). This loss of potency of the oncolytic AdAM7 compared to AdAM8 is therefore likely to be due to the increased size of the adenoviral genome containing the NIS coding sequence compared to its gp19k-deleted (AdAM8). The relationship between adenoviral genome size and viral yield has already been studied in great detail [44–46]. The NIS cDNA is around 2 kb in size and this extra burden of viral DNA may be responsible for the lower virus yield obtained following infection of IGROV-1 cells (Fig. 3a).

In vivo imaging of AdAM7 propagation following intraperitoneal injection in icodextrin demonstrated that NIS expression was maximal 48 h after virus administration and undetectable 8 days after administration (Fig. 5). The transient nature of these kinetics is reminiscent of those obtained following intratumoral injection of other oncolytic adenoviruses in other settings. In immunocompetent mice, tumours injected with a replication-selective adenovirus show a peak of NIS expression 48 h after oncolytic virus

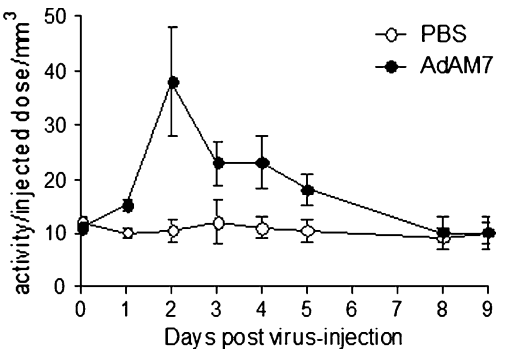

Fig. 5 Quantification of hNIS-dependent intraperitoneal $^{99m}TcO_4^-$ accumulation in vivo. Mice bearing intraperitoneal IGROV-luc tumour deposits were injected into the peritoneal cavity in the presence of icodextrin with PBS or 10^{10} particles/mouse of AdAM7. On the days indicated, mice were injected with 18.5 MBq of $^{99m}TcO_4^-$ and imaged. Radioisotope accumulation was quantified using InVivoScope and the results are presented as $^{99m}TcO_4^-$ activity per injected dose per mm^3 of tumour volume. There were four mice treated with AdAM7 and three mice treated with PBS

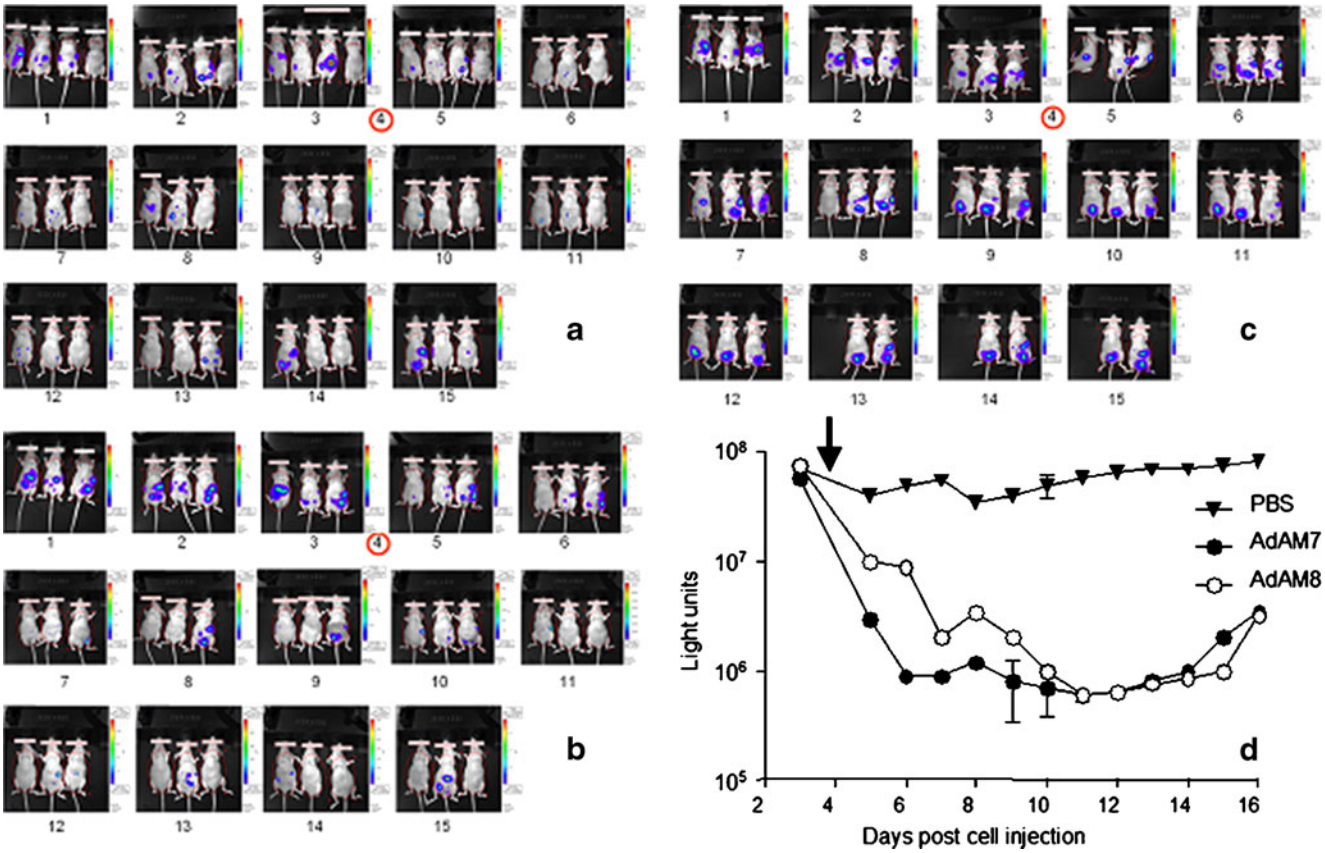

Fig. 6 Comparison of the therapeutic efficacy of AdAM7 and AdAM8. Balb-c nude mice were seeded intraperitoneally with IGROV-luc cells. Four days later (*arrows*), mice were injected with PBS (n=4), or 10^{10} particles of AdAM7 (n=4) or AdAM8 (n=4). Tumour burden was measured on different days (as indicated) by measuring the luciferase activity in the peritoneal cavity. **a**–**c** Examples of bioluminescence imaging of tumour burdens in mice treated with AdAM7 (**a**), AdAM8 (**b**) and PBS (**c**). **d** Quantification of the bioluminescence imaging in all experimental mice. The data represent the means±SD of the tumour measurements, and are representative of two experiments

administration, followed by a sharp disappearance of *hNIS*-dependent accumulation of radiotracer [9]. In patients, intraprostatic administration of a replication-selective adenovirus has been shown to lead to a peak of NIS expression 1–2 days after administration and is detectable in the prostate for up to 7 days [26]. In this context, our data confirm that NIS expression mediated by an oncolytic adenovirus is transient and that the peak is also reached rapidly (2 to 3 days after administration) when the virus is administered intraperitoneally instead of intratumorally. Furthermore, NIS expression was only detectable in the peritoneal cavity (Fig. 5).

The differences between the observations in the in vitro experiments (Fig. 3) and in vivo experiments (Fig. 5) were in our view due to differences in the conditions of the experiments. In vitro, the virus is added to the cells and the viral progeny produced after viral replication and lysis of the cell is released into the culture medium. A large proportion of the virus has access to uninfected cells, that will produce more virus following infection. This process will repeat itself until all the cells are destroyed. Our data (Fig. 3) show that under the conditions of the experiment, the bulk of infective virus production was reached 48 h after infection and the titre of the virus stayed stable for at least another 2 days. In the in vivo situation, the virus released after destruction of the infected cells can also infect neighbouring cells but this virus can also diffuse away from the peritoneal cavity in the general circulation. This phenomenon has been described in detail by Johnson et al. [42]. As a result, fewer cells will be infected and the signal will gradually disappear.

In terms of therapeutic effect in vivo, no statistically significant difference was observed between the tumour burdens of AdAM7- and AdAM8-treated animals (Fig. 6). This is in sharp contrast with the situation in vitro in which AdAM7 was less cytotoxic than AdAM8 (Fig. 4). Considering that this reduced cytotoxicity in vitro is likely to have resulted from a reduced capacity of AdAM7 to replicate in IGROV-1 cells compared to AdAM8 and that in vivo NIS expression was only transiently detected 2 and 3 days after virus administration, we suggest that adenoviral oncolysis is achieved rapidly after virus inoculation, as opposed to

delayed and mediated by several rounds of autoamplification of the virus.

In conclusion, we demonstrates in this study that infection of intraperitoneal cancer cells following intraperitoneal administration of an oncolytic adenovirus can be monitored in vivo using *NIS* as a reporter gene. Although insertion of the *NIS* coding sequence in the viral genome has deleterious effects on its cytotoxicity in vitro, no difference in therapeutic efficacy was observed in vivo, suggesting that *NIS* is a highly relevant reporter gene to monitor the fate of oncolytic adenovectors in the live subject.

Acknowledgments The authors would like to thank Dr. Jhiang for providing the human NIS cDNA. This work was supported by grants from Cancer Research UK, the Medical Research Council, INSERM, la Ligue Nationale Contre le Cancer, the "Paris scientifiques régionaux" scheme of the Région Pays de la Loire, and the French National Cancer Institute (INCa, grant 0607-3D1615-66/AO INSERM).

References

1. Baril P, Martin-Duque P, Vassaux G. Visualization of gene expression in the live subject using the Na/I symporter as a reporter gene: applications in biotherapy. Br J Pharmacol 2009. doi:10.1111/j.1476-5381.2009.00412.x.
2. Dadachova E, Carrasco N. The Na/I symporter (NIS): imaging and therapeutic applications. Semin Nucl Med 2004;34:23–31.
3. Vassaux G, Groot-Wassink T. In vivo noninvasive imaging for gene therapy. J Biomed Biotechnol 2003;2003:92–101.
4. Serganova I, Ponomarev V, Blasberg R. Human reporter genes: potential use in clinical studies. Nucl Med Biol 2007;34:791–807.
5. Faivre J, Clerc J, Gerolami R, et al. Long-term radioiodine retention and regression of liver cancer after sodium iodide symporter gene transfer in wistar rats. Cancer Res 2004;64:8045–51.
6. Marsee DK, Shen DH, MacDonald LR, et al. Imaging of metastatic pulmonary tumors following NIS gene transfer using single photon emission computed tomography. Cancer Gene Ther 2004;11:121–7.
7. Shah K, Jacobs A, Breakefield XO, Weissleder R. Molecular imaging of gene therapy for cancer. Gene Ther 2004;11:1175–87.
8. Dohan O, Carrasco N. Advances in Na(+)/I(-) symporter (NIS) research in the thyroid and beyond. Mol Cell Endocrinol 2003;213:59–70.
9. Merron A, Peerlinck I, Martin-Duque P, et al. SPECT/CT imaging of oncolytic adenovirus propagation in tumours in vivo using the Na/I symporter as a reporter gene. Gene Ther 2007;14:1731–8.
10. Groot-Wassink T, Aboagye EO, Glaser M, Lemoine NR, Vassaux G. Adenovirus biodistribution and noninvasive imaging of gene expression in vivo by positron emission tomography using human sodium/iodide symporter as reporter gene. Hum Gene Ther 2002;13:1723–35.
11. Groot-Wassink T, Aboagye EO, Wang Y, Lemoine NR, Keith WN, Vassaux G. Noninvasive imaging of the transcriptional activities of human telomerase promoter fragments in mice. Cancer Res 2004;64:4906–11.
12. Groot-Wassink T, Aboagye EO, Wang Y, Lemoine NR, Reader AJ, Vassaux G. Quantitative imaging of Na/I symporter transgene expression using positron emission tomography in the living animal. Mol Ther 2004;9:436–42.
13. Chisholm EJ, Vassaux G, Martin-Duque P, et al. Cancer-specific transgene expression mediated by systemic injection of nanoparticles. Cancer Res 2009;69:2655–62.
14. Kim HJ, Jeon YH, Kang JH, et al. In vivo long-term imaging and radioiodine therapy by sodium-iodide symporter gene expression using a lentiviral system containing ubiquitin C promoter. Cancer Biol Ther 2007;6:1130–5.
15. Kim KI, Chung JK, Kang JH, et al. Visualization of endogenous p53-mediated transcription in vivo using sodium iodide symporter. Clin Cancer Res 2005;11:123–8.
16. Yeom CJ, Chung JK, Kang JH, et al. Visualization of hypoxia-inducible factor-1 transcriptional activation in C6 glioma using luciferase and sodium iodide symporter genes. J Nucl Med 2008;49:1489–97.
17. Che J, Doubrovin M, Serganova I, et al. HSP70-inducible hNIS-IRES-eGFP reporter imaging: response to heat shock. Mol Imaging 2007;6:404–16.
18. Kim KI, Kang JH, Chung JK, et al. Doxorubicin enhances the expression of transgene under control of the CMV promoter in anaplastic thyroid carcinoma cells. J Nucl Med 2007;48:1553–61.
19. Chen L, Altman A, Mier W, Lu H, Zhu R, Haberkorn U. 99mTc-pertechnetate uptake in hepatoma cells due to tissue-specific human sodium iodide symporter gene expression. Nucl Med Biol 2006;33:575–80.
20. Hwang DW, Jang SJ, Kim YH, et al. Real-time in vivo monitoring of viable stem cells implanted on biocompatible scaffolds. Eur J Nucl Med Mol Imaging 2008;35:1887–98.
21. Lee KH, Bae JS, Lee SC, et al. Evidence that myocardial Na/I symporter gene imaging does not perturb cardiac function. J Nucl Med 2006;47:1851–7.
22. Boland A, Ricard M, Opolon P, et al. Adenovirus-mediated transfer of the thyroid sodium/iodide symporter gene into tumors for a targeted radiotherapy. Cancer Res 2000;60:3484–92.
23. Montiel-Equihua CA, Martin-Duque P, de la Vieja A, et al. Targeting sodium/iodide symporter gene expression for estrogen-regulated imaging and therapy in breast cancer. Cancer Gene Ther 2008;15:465–73.
24. Goel A, Carlson SK, Classic KL, et al. Radioiodide imaging and radiovirotherapy of multiple myeloma using VSV(Delta51)-NIS, an attenuated vesicular stomatitis virus encoding the sodium iodide symporter gene. Blood 2007;110:2342–50.
25. Peerlinck I, Merron A, Baril P, et al. Targeted radionuclide therapy using a Wnt-targeted replicating adenovirus encoding the Na/I symporter. Clin Cancer Res 2009;15:6595–601.
26. Barton KN, Stricker H, Brown SL, et al. Phase I study of noninvasive imaging of adenovirus-mediated gene expression in the human prostate. Mol Ther 2008;16:1761–9.
27. Kaplan JM. Adenovirus-based cancer gene therapy. Curr Gene Ther. 2005;5:595–605.
28. Woo Y, Adusumilli PS, Fong Y. Advances in oncolytic viral therapy. Curr Opin Investig Drugs 2006;7:549–59.
29. Fueyo J, Gomez-Manzano C, Alemany R, et al. A mutant oncolytic adenovirus targeting the Rb pathway produces anti-glioma effect in vivo. Oncogene 2000;19:2–12.
30. Gomez-Manzano C, Alonso MM, Yung WK, et al. Delta-24 increases the expression and activity of topoisomerase I and enhances the antiglioma effect of irinotecan. Clin Cancer Res 2006;12:556–62.
31. Lockley M, Fernandez M, Wang Y, et al. Activity of the adenoviral E1A deletion mutant dl922-947 in ovarian cancer: comparison with E1A wild-type viruses, bioluminescence monitoring, and intraperitoneal delivery in icodextrin. Cancer Res 2006;66:989–98.
32. Dingli D, Peng KW, Harvey ME, et al. Image-guided radiovirotherapy for multiple myeloma using a recombinant measles

virus expressing the thyroidal sodium iodide symporter. Blood 2004;103:1641–6.
33. Peerlinck I, Amini-Nik S, Phillips RK, et al. Therapeutic potential of replication-selective oncolytic adenoviruses on cells from familial and sporadic desmoid tumors. Clin Cancer Res 2008;14:6187–92.
34. Gagnebin J, Brunori M, Otter M, Juillerat-Jeanneret L, Monnier P, Iggo R. A photosensitising adenovirus for photodynamic therapy. Gene Ther 1999;6:1742–50.
35. Vassaux G, Manson AL, Huxley C. Copy number-dependent expression of a YAC-cloned human CFTR gene in a human epithelial cell line. Gene Ther 1997;4:618–23.
36. Coughlan L, Vallath S, Saha A, et al. In vivo retargeting of adenovirus type 5 to alphavbeta6 integrin results in reduced hepatotoxicity and improved tumor uptake following systemic delivery. J Virol 2009;83:6416–28.
37. Martin-Duque P, Jezzard S, Kaftansis L, Vassaux G. Direct comparison of the insulating properties of two genetic elements in an adenoviral vector containing two different expression cassettes. Hum Gene Ther 2004;15:995–1002.
38. Hingorani M, White CL, Merron A, et al. Inhibition of repair of radiation-induced DNA damage enhances gene expression from replication-defective adenoviral vectors. Cancer Res 2008;68:9771–8.
39. Aoi A, Watanabe Y, Mori S, Takahashi M, Vassaux G, Kodama T. Herpes simplex virus thymidine kinase-mediated suicide gene therapy using nano/microbubbles and ultrasound. Ultrasound Med Biol 2008;34:425–34.
40. Briat A, Vassaux G. A new transgenic mouse line to image chemically induced p53 activation in vivo. Cancer Sci 2008;99:683–8.
41. Baird SK, Aerts JL, Eddaoudi A, Lockley M, Lemoine NR, McNeish IA. Oncolytic adenoviral mutants induce a novel mode of programmed cell death in ovarian cancer. Oncogene 2008;27:3081–90.
42. Johnson M, Huyn S, Burton J, Sato M, Wu L. Differential biodistribution of adenoviral vector in vivo as monitored by bioluminescence imaging and quantitative polymerase chain reaction. Hum Gene Ther 2006;17:1262–9.
43. Page JG, Tian B, Schweikart K, et al. Identifying the safety profile of a novel infectivity-enhanced conditionally replicative adenovirus, Ad5-delta24-RGD, in anticipation of a phase I trial for recurrent ovarian cancer. Am J Obstet Gynecol 2007;196:389 e1–9; discussion e9–10.
44. Bett AJ, Prevec L, Graham FL. Packaging capacity and stability of human adenovirus type 5 vectors. J Virol 1993;67:5911–21.
45. Parks RJ, Graham FL. A helper-dependent system for adenovirus vector production helps define a lower limit for efficient DNA packaging. J Virol 1997;71:3293–8.
46. Kennedy MA, Parks RJ. Adenovirus virion stability and the viral genome: size matters. Mol Ther 2009;17:1664–6.